



## Research Article

# Modification of Soluble Dietary Fiber from Millet by Selenylation and Its Immune-Enhancing Activity

Yunfei Ge <sup>1</sup>, Chunhong Wei,<sup>1,2</sup> Dezhi Liu,<sup>1</sup> and Longkui Cao <sup>1,2</sup>

<sup>1</sup>College of Food Science, Heilongjiang Bayi Agricultural University, Xinfeng Lu 5, Daqing 163319, China

<sup>2</sup>National Coarse Cereals Engineering Research Center, Heilongjiang Bayi Agricultural University, Daqing 163319, China

Correspondence should be addressed to Longkui Cao; caolongkui2013@163.com

Received 16 June 2023; Revised 14 August 2023; Accepted 28 August 2023; Published 12 September 2023

Academic Editor: Akhilesh K. Verma

Copyright © 2023 Yunfei Ge et al. This is an open access article distributed under the Creative Commons Attribution License, which permits unrestricted use, distribution, and reproduction in any medium, provided the original work is properly cited.

The immune activity of polysaccharides increases after structural modification, whereas the structure of dietary fiber is similar to that of polysaccharides, and research on the chemical modification of dietary fiber is lacking. Therefore, in this study, we used soluble dietary fiber from millet to chelate metal selenium ions, named the selenium-enriched additive (SDF-Se), and investigated its effects on macrophages and natural killer (NK) cells *in vitro*. The results showed that SDF-Se could activate RAW 264.7 cells through NF- $\kappa$ B and mitogen-activated protein kinase (MAPK) signaling and promote the accumulation of the reactive oxygen species, thereby increasing the levels of TNF- $\alpha$ , IL-6, and IL-10 and releasing numerous NO molecules. Furthermore, SDF-Se treatment induced NK cells to secrete cytokines (IFN- $\gamma$  and TNF- $\alpha$ ), cytoplasmic granules (granzyme-B), surface-activating receptors (NKP44), and increased CD56 and CD107a expressions, which promote NK cell cytotoxic responses. These results suggest that SDF-Se can promote macrophage and NK cell activation and be used as a potent immunostimulant.

## 1. Introduction

Selenium, a trace element, is involved in several crucial metabolic pathways in the body. Low levels of selenium are positively correlated with a high risk of cancer, heart disease, hyperlipidemia, and hypertension [1, 2]. As a result, proper selenium supplementation in daily life not only reduces the risk of cancer but also has antioxidant, antiviral, and anti-aging effects [3–5] and plays an essential role in the activation, proliferation, and differentiation of immune cells [6]. Thus, owing to its unique properties, selenium is increasingly being investigated as a promising candidate for future medicines and functional foods. The presence of selenium in two primary forms, organic and inorganic selenium, makes the dosage of inorganic selenium difficult to control, limiting its application [7]. Organic selenium in the form of selenoproteins or selenopolysaccharides has low toxicity, high activity, and high bioavailability and can effectively stimulate the immune response [8, 9]. Therefore, combining selenium with specific active ingredients is an effective method for improving its utilization.

Dietary fiber, the seventh macronutrient, can be degraded and utilized by microbial fermentation in the large intestine, but it is more difficult to digest and absorb in the small intestine. Dietary fiber is classified as insoluble and soluble based on its water-soluble quality [10, 11]. Soluble dietary fiber (SDF) receives the most attention owing to its essential role in reducing hunger, promoting digestion, and controlling blood sugar levels [12]. In addition, SDF has a high utilization value and can be used as a food additive owing to its physical, chemical, and functional properties [13]. Relevant studies have shown that the structure of dietary fiber can be modified to improve its biological activity [14], but studies on the modification of soluble dietary fibers and chelation of metal ions are insufficiently reported. The structure of SDF is similar to that of polysaccharides, and related studies have demonstrated that when polysaccharides are chelated with metal selenium ions, the complexes have higher biological activity than polysaccharides or the selenium ion alone [15]. As a result, chelating soluble dietary fibers with the metal Se ion to synthesize the selenium-enriched additive (SDF-Se) is not

only an effective method for developing new selenium sources but can also optimize the physiopharmacological functions of selenium and polysaccharides. Consequently, investigating the biosynthesis and immunological activity of selenized SDF has far-reaching implications.

Millet, a traditional Chinese cereal, has high nutritional value, gets easily digested, and has a strong nutritional effect on human gastrointestinal diseases, piquing the interest of researchers. In our laboratory, we used the sodium nitrate-selenite method to obtain selenite millet SDF; under optimal selenization modification conditions, the yield of millet SDF-Se was 10.56%, and the selenium content was 2.69 mg/g. Following modification, the molecular mass of millet SDF-Se increased, and the surface was porous with a large pore size and honeycomb shape, which also enhanced the *in vitro* antioxidant capacity and improved the *in vivo* colitis-related inflammation [16]. The prevalence of selenium deficiencies has been steadily increasing, resulting in immune deficiency diseases. Therefore, developing selenium-enriched products to strengthen immunity has implications for future research.

In this study, SDF was extracted using water extraction and alcohol deposition and chelated with metallic selenium ions to obtain the beneficial SDF-Se. The *in vitro* effects of SDF-Se on macrophages (RAW 264.7) and NK cells were evaluated to provide a theoretical basis and data to support the development of a new dietary fiber immune fortification agent.

## 2. Materials and Methods

**2.1. Materials and Chemicals.** Millet was purchased from Dongfang Liang Life Science and Technology Co., Inc. (Shanxi, China). All of the chemicals and reagents used in this study were of analytical grade. 5-fluorouracil (5-FU were dissolved in the 100% dimethyl sulfoxide to get the 1 mg/mL stock solution) and EZ-Cytox new cell viability assay kit (high sensitive water-soluble tetrazolium salt) were purchased from Beyotime Institute of Biotechnology (Shanghai, China). Phosphate-buffered saline (PBS), fetal bovine serum (FBS), horse serum, IL-2 recombinant human, and penicillin were purchased from Damao Chemical Reagent Factory (Tianjin, China). Roswell Park Memorial Institute (RPMI)-1640 and  $\alpha$ -MEM were purchased from Qingdao Hi-Tech Park Haibo Biotechnology Co., Ltd. Rabbit monoclonal antibodies against phosphorylated-ERK at Thr202/Tyr204 (p-ERK) #9301 (9301S), phosphorylated-P38 at Thr180/Tyr182 (p-p38) #9211 (9211S), phosphorylated-SAPK/JNK at Thr183/Tyr185 (p-JNK) #4668 (4668T), phosphorylated-P65 (p-p65) #3033 (3033S), and  $\alpha$ -tubulin (2144S) were purchased from Cell Signaling Technology, Inc. (Beverly, MA, USA). Anti-toll-like receptor 2 (anti-TLR2) (ab209216), anti-TLR4 (ab22048), and anti-CR3 (ab119347) antibodies were obtained from Abcam (Cambridge, MA, USA). High-temperature amylase, neutral protease, and amyloglucosidase were purchased from Sigma-Aldrich, USA.

**2.2. The Preparation of SDF from Millet.** The millet was crushed, passed through a 60-mesh sieve, defatted, and dried. 5 g of defatted millet powder was weighed, 125 mL of

distilled water and 250 mL of phosphate buffer solution (pH = 6, 0.08 mol/L) were added, and high-temperature resistant  $\alpha$ -amylase (95°C, 30 min), neutral protease (60°C, 30 min), and amyloglucosidase (60°C, 30 min) were used for enzymatic digestion (100°C, 20 min) for the enzyme inactivation. The reaction solution was filtered, and the filtrate was concentrated, alcohol-sedimented with four times the volume of a 95% (v/v) ethanol solution, centrifuged, and dried to obtain crude millet SDF. The Sevag reagent was prepared with V (*n*-butanol): V (trichloromethane) = 1:5 for protein removal using the Sevag method. The Sevag reagent (20 mL) was added, shaken for 10 min, and centrifuged (130000  $\times g$ , 10 min), and the aqueous phase was collected. The Sevag reagent (20 mL) was added to the aqueous phase, shaken, and centrifuged, and the aqueous phase was collected again; the abovementioned steps were repeated 10 times. The final collected aqueous phase was adjusted with 5% v/v ammonia to pH 8.5 and 50 mL of 30% hydrogen peroxide was added and decolorized at 40°C for 60 min, and the organic reagents were removed by rotary evaporation at 60°C to obtain approximately 20 mL of millet SDF solution. The procedures that were performed to obtain the purified millet SDF were dialysis, concentration, addition of 4 times the volume of 95% ethanol solution, alcoholic sedimentation overnight in a refrigerator at 4°C, discarding the supernatant, centrifugation (130000  $\times g$ , 10 min), washing the precipitate twice with anhydrous ethanol and acetone, and was freeze-dried [17].

**2.3. The Preparation of the Millet SDF-Se Complex.** This study was performed as described in the reference to prepare the millet SDF-Se [18]. An amount of 500 mg of millet SDF was weighed, and 50 mL of a 0.5% v/v HNO<sub>3</sub> solution was slowly added dropwise and constantly stirred for complete dissolution. It was stirred in 0.65 g of barium chloride and 3 mL of sodium selenite solution (5 mg/mL) for 6 h at 40°C. After cooling the reaction solution, the pH was adjusted to 5-6 with 20% sodium carbonate solution, sodium sulfate was added to remove the barium ions, centrifugation was performed for 10 min at 130000  $\times g$ , the supernatant was collected, and dialysis was performed to remove sodium selenite. The dialysis solution was taken with ascorbic acid every 6 h to detect the residual amount of free sodium selenite, and the dialysis was stopped when no red color appeared. To obtain millet SDF-Se, the dialysis solution was concentrated to 10–20 mL, desalted via dialysis with distilled water for 24 h, and freeze-dried.

**2.4. Cell Line and Cell Culture.** The murine macrophage RAW 264.7, NK, and HeLa cell lines were obtained from the Cell Bank of Shanghai Institutes for Biological Sciences, Chinese Academy of Sciences (Shanghai, China). RAW 264.7 macrophages and HeLa cells were cultured in the RPMI-1640 medium supplemented with 10% FBS, 100 U/mL of penicillin, and 100  $\mu$ g/mL streptomycin. The NK cell was cultured in the  $\alpha$ -MEM medium that was supplemented with 10% FBS, 10% horse serum, 0.2 mM inositol, 0.02 mM folic acid, 0.1 mM  $\beta$ -mercaptoethanol, and 10 ng/mL IL-2.

The culture was maintained at 37°C with 5% CO<sub>2</sub> (ESPEC CO<sub>2</sub> incubator).

**2.5. Cell Proliferation and Nitric Oxide (NO) Production Assay.** RAW 264.7, NK, and HeLa cells were seeded in a 96-well plate (1 × 10<sup>6</sup> cells/mL) and incubated at 37°C for 24 h in a CO<sub>2</sub> incubator. Then, the cells were individually treated with different concentrations of SDF, SDF-Se (50, 100, and 200 µg/mL), or LPS (2 µg/mL; positive control); medium was used as a negative control. After incubation at 37°C for 18 h, the NO production and cell proliferation were determined using the Griess reaction and EZ-Cytox new cell viability assay kit. The amount of NO produced by macrophages was quantified using NaNO<sub>2</sub> (1 µM–200 µM in the culture medium) [19, 20].

**2.6. Coculture Cytotoxicity Assay.** NK cells were treated with the SDF or SDF-Se at different concentrations (50–200 µg/mL) for 24 h; medium was used as a negative control. The activated-NK cells were transferred to HeLa cells (4 × 10<sup>4</sup> cells/mL) using effector: target cell ratios (E: T) (NK: HeLa) of 25:1. The experiment was repeated in triplicate. The plate was incubated at 37°C under 5% CO<sub>2</sub> atmosphere. After incubation for 4 h, the EZ-Cytox new cell viability assay kit was used to detect the cytotoxicity, and the plate was incubated for an additional 45 min. The OD values were recorded at 450 nm, using a microplate reader (EL-800, BioTek Instruments, Winooski, VT, USA). The cytotoxicity was expressed as ratios according to the following formula:

$$\text{Cytotoxicity (\%)} = 100 \left( 1 - \left( \frac{A_s}{A_m} \right) \right), \quad (1)$$

where “As” is the absorbance of the sample and “Am” is the absorbance of the medium.

In addition, the cytotoxicity was confirmed by counting the live cells obtained from a confocal quantitative image cytometer (CQ1, Yokogawa, Tokyo, Japan)

**2.7. Real-Time PCR Assay.** RAW 264.7 cells and NK cells were seeded in a 24-well microplate (1 × 10<sup>6</sup> cells/mL) and were cultured for 24 h in the presence of the SDF, SDF-Se (50, 100, and 200 µg/mL), or LPS (2 µg/mL; positive control) and medium was used as a negative control. Total RNA was extracted using TRIzol reagent (Takara, Kusatsu, China), and the concentration of RNA was measured before constructing cDNA with an oligo-(dT) 20 primer and superscript III RT (Takara). The primers used are shown in Table 1, and β-actin was used as the internal standard. Real-time PCR reactions were performed using the CFX Connect Real-Time System (Bio-Rad Hercules, CA, USA) with a Fast Start DNA Master TB Green II kit, and the results were expressed relative to β-actin [10].

**2.8. ROS Generation Assay.** There are numerous methods for detecting intracellular reactive oxygen species (ROS), with DCFH-DA being one of the most widely used probes for determining intracellular redox status. RAW 264.7 cells were

TABLE 1: The detail of primers used in the real-time PCR analysis.

Gene		Primer sequence
iNOS	Forward	CTGCAGCACTTGGATCAGGAACCT G
	Reverse	GGGAGTAGC CTGTGTGCACCTGGAA
IL-1β	Forward	ATGGCAACTATTCCAGAACTCAAC T
	Reverse	CAGGACAGGTATAGATTCTTTCCT TT
IL-6	Forward	TTCTCTCTGCAAGAGACT
	Reverse	TGTATCTCTCTGAAGGACT
IL-10	Forward	TACCTGGTAGAAGTGATGCC
	Reverse	CATCATGTATGCTTCTATGC
TNF-α	Forward	CCCCACAGTCAAAGACACT
	Reverse	TACAGGCTTGCACTCGAATT
IFN-γ	Forward	GATGCTCTTCGACCTCGAAACAGC AT
	Reverse	ATGAAATATACAAGTTATAATCTT GGCTTT
Granzyme-β	Forward	AGATCGAAAGTGCGAATCTGA
	Reverse	TTCGTCCATAGGAGACAATGC
NKp44	Forward	TCCAAGGCTCAGGTACTTCAA
	Reverse	GAT-TGTGAATCGAGAGGTCCA
β-Actin	Forward	ATGTGCAAAAAGCTGGCTTTG
	Reverse	ATTTGTGGTGGATGATGGAGG

seeded in a 24-well plate (5 × 10<sup>5</sup> cells/mL), cultured in a 5% CO<sub>2</sub> incubator for 24 h, and treated with SDF, SDF-Se (200 µg/mL), or LPS (2 µg/mL; positive control) for 24 h, medium was used as a negative control, and DCFH-DA was used to detect ROS production. The cells were collected and reacted in DCFH-DA at 37°C for 45 min while being shielded from light. PBS was used to wash the cells three times. Using a fluorescence microscope, the production of ROS was observed.

**2.9. Flow Cytometry Assay.** RAW 264.7 cells (1 × 10<sup>6</sup> cells/mL) and NK cells were cultured for 24 h in a 6-well plate, treated with SDF, SDF-Se (200 µg/mL), or LPS (2 µg/mL; positive control) for 24 h, and medium was used as a negative control, and then the cell was harvested and washed with FACS buffer containing 1% bovine serum albumin and 0.1% sodium azide. Subsequently, the cells were stained with antibodies for 30 min at 4°C. Parallel sets of cells were incubated without the antibodies, and their autofluorescence intensity served as a nonspecific negative control. A total of 100,000 viable cells per treatment (as determined using light scatter profiles) were analyzed using a FACS flow cytometer (BD, Franklin Lakes, NJ, USA) [10].

**2.10. Western Blot Assay.** RAW 264.7 cells (2 × 10<sup>6</sup> cells/mL) were cultured for 24 h in the presence of the SDF-Se (50–200 µg/mL) or LPS (2 µg/mL), medium as a control, and then the cells were washed three times with PBS, and the protein was extracted using lysis reagents (1 mL RIPA lysis buffer + 1 µL inhibitor cocktail + 1 µL EDTA). The protein

content was measured using a BCA protein assay kit. The extracted protein was loaded, separated using 10% sodium dodecyl sulfate-polyacrylamide gel electrophoresis, and then transferred onto a polyvinylidene fluoride membrane (0.22  $\mu\text{m}$ ; Millipore, Burlington, MA, USA). The membranes were incubated with primary antibodies at 4°C overnight after blocking with Blocking One (Nacalai Tesque, Kyoto, Japan) for 1 h. Finally, the membranes were incubated for 1 h at room temperature with horseradish peroxidase-coupled secondary antibodies. Antibodies for western blotting were diluted in 5% skim milk solution at a 1:2000 dilution from a 1 mg/mL stock solution. An enhanced chemiluminescence kit was used to detect the protein bands (Bio-Rad) [10].

**2.11. Binding Receptor Assay.** The RAW 264.7 cells were pretreated with 10  $\mu\text{g}/\text{mL}$  of anti-TLR2, TLR4, and anti-CR3 antibodies before the treatment of SDF-Se. The production of the NO content was assessed by the procedure mentioned in Section 2.5.

**2.12. Statistical Analysis.** Excel 2016 and SPSS 19.0 software were used for the statistical analysis of the data; Origin 8.0 software was used for drawing processing, and the data were measured in triplicate to obtain the average value. The results are presented as the mean + SD. The significance was calculated by one-way ANOVA.  $p < 0.05$  was considered statistically significant and  $p < 0.01$  was extremely significant (\*  $p < 0.05$ , \*\*  $p < 0.01$ , and \*\*\*  $p < 0.001$ ).

### 3. Results

#### 3.1. The Effects of SDF-Se on the Activation of RAW 264.7 Cells

**3.1.1. The Effects of SDF and SDF-Se on Cell Proliferation and NO Production.** As depicted in Figure 1(a), SDF and SDF-Se presented no significant inhibitory effect on macrophage growth at concentrations ranging from 50 to 200  $\mu\text{g}/\text{mL}$ , whereas SDF-Se caused apoptosis of RAW 264.7 cells at 400  $\mu\text{g}/\text{mL}$ , indicating that excess selenized dietary fiber produced toxic effects on RAW 264.7 macrophages. As the principal effector molecule produced by macrophages, NO is a critical mediator of many biological functions and can be considered a critical marker of macrophage activation; thus, the magnitude of NO production demonstrated a significant positive correlation with the degree of cell activation. The Griess method was used to determine the NO production in RAW 264.7 cells, and the result is shown in Figure 1(b); SDF did not affect NO production compared with the control group (medium), but NO production was considerably higher in the SDF-Se group, indicating that SDF-Se was able to significantly induce NO secretion in a dose-dependent manner.

**3.1.2. The Effects of SDF and SDF-Se on the mRNA Expression of Inflammatory Factors.** The real-time polymerase chain reaction (RT-PCR) was used to investigate the effect of SDF and SDF-Se on the mRNA expression of inflammatory factors on RAW 264.7 cells, and the results are shown in

Figure 2. Millet soluble dietary fiber (SDF) did not significantly affect the mRNA expression of inflammatory factors, but the relative expression of TNF- $\alpha$  (4.21-fold), iNOS (4.80-fold), IL-1 $\beta$  (7.63-fold), IL-10 (4.54-fold), and IL-6 (8.00-fold) mRNAs in the SDF-Se group following modification were significantly higher than that of the control group (medium) with the high concentration ( $p < 0.01$ ), and their expressions increased with sample concentration.

**3.1.3. The Effect of SDF and SDF-Se on the Reactive Oxygen Species Generation.** Reactive oxygen species (ROS) are normal metabolites of redox reactions in normal cells that play a crucial role in immune regulation. Therefore, we investigated the accumulation of ROS in RAW 264.7 cells induced by SDF and SDF-Se to further demonstrate their effect on immune cell activation (Figure 3). When RAW 264.7 cells were incubated with SDF, SDF-Se, or LPS for 24 h, the fluorescence intensity in the cells treated with SDF-Se and LPS increased compared to that in the control group (medium), indicating that selenium ions enhance SDF immune activity, which in turn mediates ROS accumulation in macrophages.

**3.1.4. The Effect of SDF and SDF-Se on the Expression of Surface Molecules in RAW 264.7 Cells.** Because the expression of surface molecules, such as CD11b and CD40, which are significant of macrophage activation, was discovered to be positively correlated with cell activation, this experiment was performed to investigate the expression of surface molecules such as CD11b and CD40 using cell flowmetry. The experimental results are shown in Figure 4; both SDF and SDF-Se stimulated the expression of macrophage surface molecules CD11b and CD40 when compared to the control group (medium), but there were intergroup differences, with SDF-Se having significantly higher molecular upregulation than SDF, indicating that selenium ions could increase the immune activity of millet SDF. The expression of the inflammatory regulator CD40 did not differ significantly between the LPS and SDF-Se groups, indicating that SDF-Se exerted immunomodulatory effects by increasing the expression of surface molecules (CD11b and CD40).

**3.1.5. The Effect of SDF and SDF-Se on the Mitogen-Activated Protein Kinase and NF- $\kappa\text{B}$  Signaling Pathways.** As shown in Figure 5, SDF-Se and LPS treatment could upregulate the expression of p-p38, p-JNK, p-ERK, and p-p65 in RAW 264.7 cells, indicating that both SDF-Se and LPS could enforce macrophage immune activation by upregulating the MAPK and NF- $\kappa\text{B}$  signaling pathways.

**3.1.6. The Effect of SDF and SDF-Se on Specific Antibodies against Pattern Recognition Receptors.** RAW 264.7 cells were pretreated with an anti-CR3 antibody and cocultured with SDF-Se for 24 h. The results showed that CR3 antibody pretreatment significantly blocked NO production

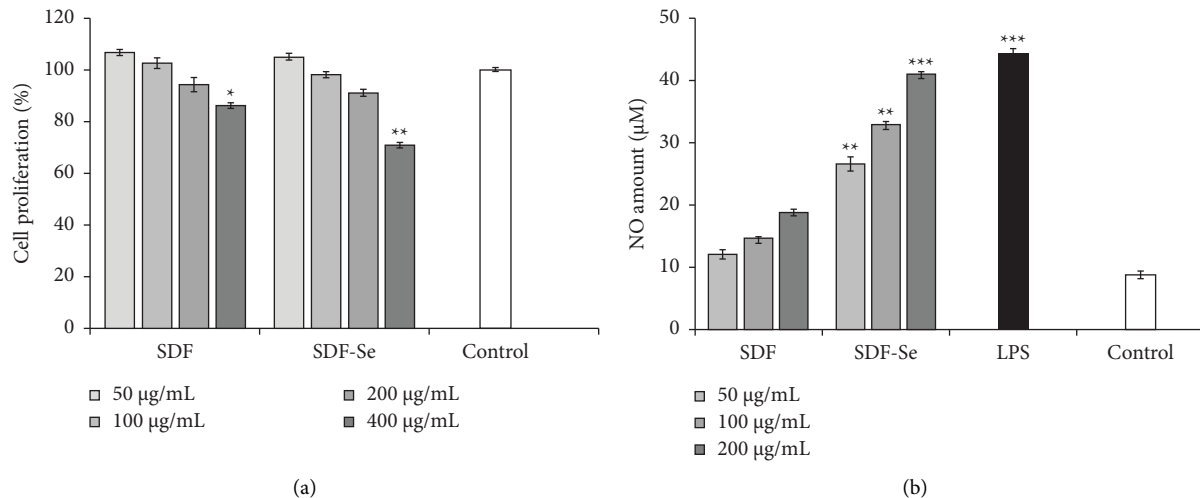


FIGURE 1: The effects of SDF and SDF-Se on cell proliferation and nitric oxide (NO) production: (a) RAW 264.7 cell proliferation was detected after exposure to different concentrations of SDF or SDF-Se (50, 100, 200, and 400, µg/mL) and (b) NO production of the RAW 264.7 cells was detected after exposure to different concentrations of SDF or SDF-Se (50, 100, and 200, µg/mL). Data are expressed as the mean ± SD. The asterisks indicate statistical changes (\*  $p < 0.05$ , \*\*  $p < 0.01$ , and \*\*\*  $p < 0.001$  versus control group).

stimulated by SDF-Se (Figure 6), implying that SDF-Se regulates the immune response by binding to CR3 receptors.

### 3.2. The Effect of SDF-Se on NK Cell Activation

**3.2.1. The Effects of SDF and SDF-Se on NK and HeLa Cell Proliferation.** Previous studies have shown that a complex of millet SDF and Se ions can activate macrophages and strengthen their immunostimulatory activity. To investigate the effects of SDF and SDF-Se on the activation of NK cells, we examined their viability on NK and HeLa cells. After 24 h of sample treatment, there was no significant difference in the viability of NK and HeLa cells when compared to the control group (medium) (Figure 7), indicating that SDF and its metal ion chelate have no toxic side effects on NK or HeLa cells, meaning we could proceed with the subsequent cytotoxicity test of NK cells on HeLa cells.

**3.2.2. The Effects of SDF and SDF-Se on NK Cell Cytotoxicity.** The results are shown in Figure 8(a); the cytotoxicity of NK cells against HeLa cancer cells was 22.58%, indicating that NK cells could directly induce apoptosis in targeted cancer cells, and SDF-Se significantly increased the cytotoxicity of NK cells compared to SDF. The NK cell cytotoxicity level was confirmed by CQ1 analysis (Figures 8(b)–8(e)) using HeLa cells cocultured with unstimulated NK cells as control, which revealed a large number of live HeLa cells after 4 h of incubation, whereas SDF-Se and 5-FU groups considerably reduced the number of live cells ( $p < 0.05$ ), implying that SDF-Se was able to enhance NK cell activation and increase the cytotoxicity to target cancer cells.

**3.2.3. The Effects of SDF and SDF-Se on mRNA Expression.** The effect of SDF and SDF-Zn on NK cell activities was tested by detecting the IFN- $\gamma$ , TNF- $\alpha$ , granzyme-B, and

NKp44 (an activating receptor) mRNA expression levels. The results are presented in Figure 9. SDF treatment exhibited a similar level of gene expression as NK cells alone (control group: medium), indicating that SDF has a weaker effect on NK cell activation. A similar trend was observed for NK cell cytotoxicity. When SDF was chelated with Se ions, the mRNA expression levels were significantly upregulated following treatment with SDF-Se compared to SDF. Therefore, Se ions substantially enhanced the capacity of SDF to promote NK cell activation.

**3.2.4. The Effect of SDF and SDF-Se on the Expression of Surface Molecules in NK Cells.** The cytotoxicity of NK cells was assessed by analyzing the expression of CD56 and CD107a after coculturing with HeLa cells (Figure 10). NK cells were pretreated with SDF or SDF-Se for 4 h, and the expression of CD56 and CD107a on the NK cell surface was increased. After SDF pretreatment, CD56 and CD107a expressions on the surface of NK cells were not significantly different from that in the control group (medium) ( $p < 0.01$ ), whereas it was notable in the SDF-Se group, indicating that SDF-Se increased the expression of CD56 and CD107a, thereby affecting the cytotoxicity of NK cells.

## 4. Discussion

As immune effector cells with defense and regulatory functions, macrophages can phagocytose foreign pathogens, microorganisms, and bacteria to initiate immune responses against foreign antigens [21]; they play a crucial role in host defense against pathogenic infections by secreting NO and cytokines to activate the immune system. Therefore, macrophages were used as a cell model in this investigation to evaluate the immunomodulatory effects of millet SDF before and after modification. The EZ-Cytox new cell viability assay results (Figure 1(a)) showed that SDF and SDF-Se had no

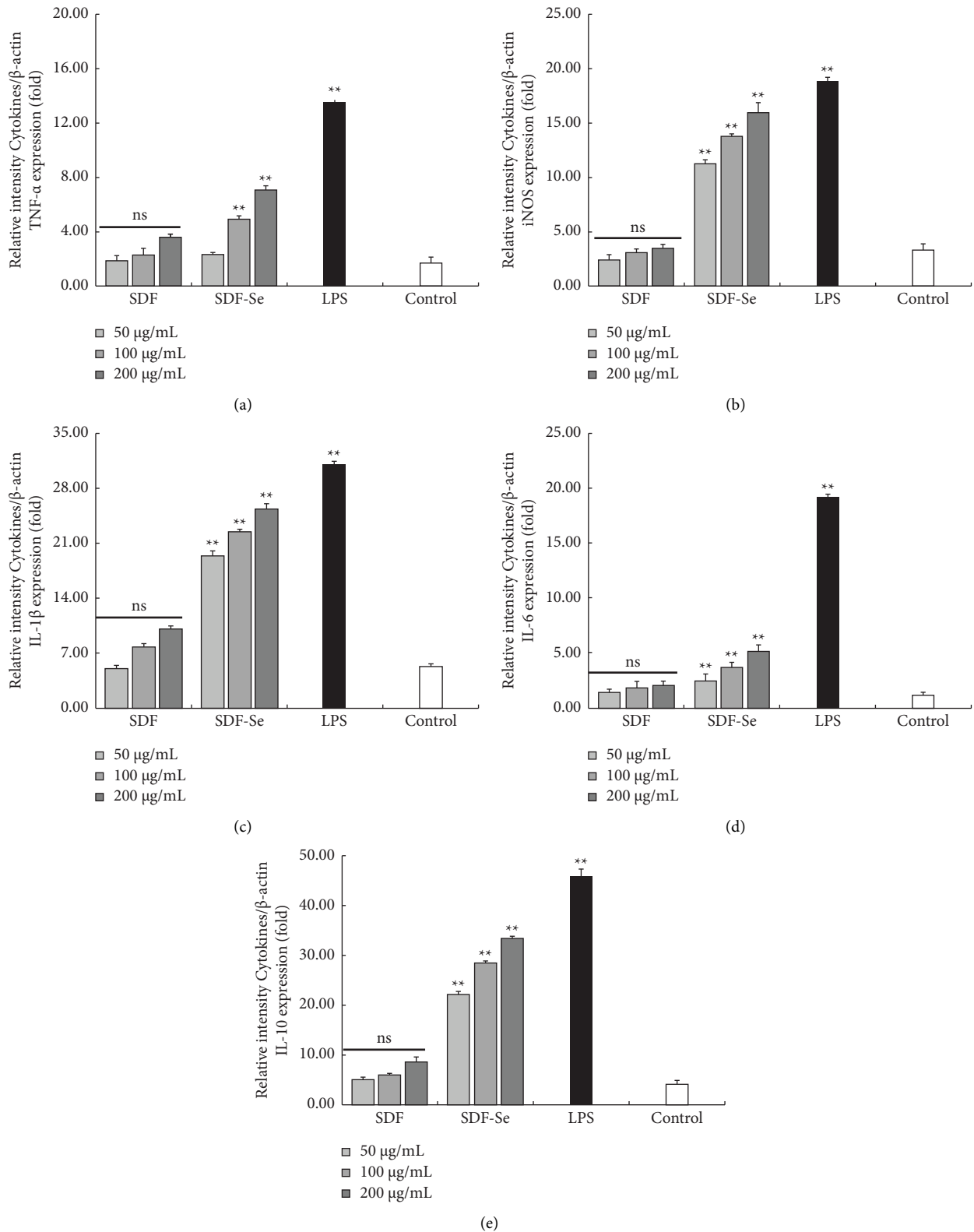


FIGURE 2: The effects of SDF or SDF-Se on mRNA expression of inflammatory factors. The RAW 264.7 cell mRNA levels were detected after exposure to different concentrations of SDF or SDF-Se (50, 100, and 200  $\mu$ g/mL). Real-time PCR was used to detect the mRNA levels of (a) TNF- $\alpha$ , (b) iNOS, (c) IL-1 $\beta$ , (d) IL-6, and (e) IL-10.  $\beta$ -Actin was used as the normalization. Data are expressed as the mean  $\pm$  SD. The asterisks indicate statistical changes (ns: not significant; \*  $p$  < 0.05, \*\*  $p$  < 0.01, and \*\*\*  $p$  < 0.001 versus control group).

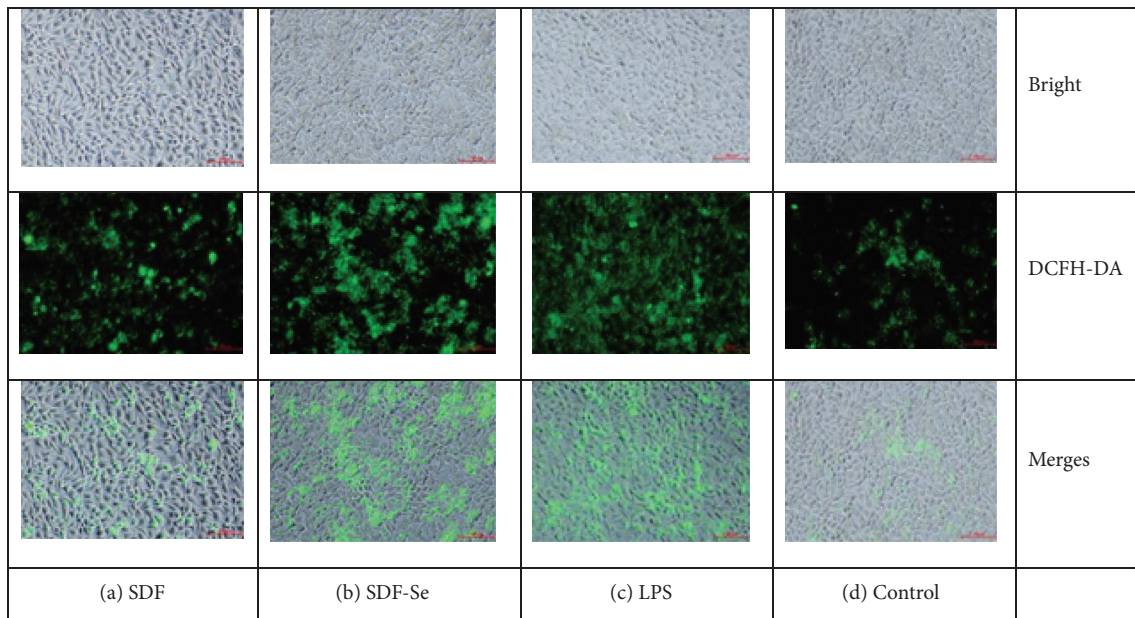


FIGURE 3: The effects of SDF or SDF-Se on ROS generation. The RAW 264.7 cells' ROS levels were detected after exposure to the SDF, SDF-Se (200  $\mu\text{g}/\text{mL}$ ), or LPS (2  $\mu\text{g}/\text{mL}$ ).

significant deleterious effects on RAW 264.7 cells at this concentration (50–200  $\mu\text{g}/\text{mL}$ ), whereas the number of macrophages and their morphology can directly reflect macrophage functions [22], indicating that both SDF and its selenide complexes can enhance RAW 264.7 cell immunity by promoting cell proliferation [23]. NO, an important messenger molecule in living cells, can stimulate a positive immune response and assist in the defense against external pathogens, such as microorganisms, viruses, bacteria, and others [23]; thus, NO can be used as an indicator of macrophage activation. To assess the immunomodulatory properties of SDF and SDF-Se, we investigated the effect of millet SDF on NO production in RAW 264.7 cells before and after selenization using the Griess assay (Figure 1(b)). In comparison to the control group (11.84  $\mu\text{M}$ ), LPS enhanced NO release (44.28  $\mu\text{M}$ ). At high concentrations, SDF may promote NO production, but it was not significantly different from the control group, and SDF-Se significantly enhanced NO secretion up to 40.90  $\mu\text{M}$  at a dose of 200  $\mu\text{g}/\text{mL}$ , which was similar to the positive control group (LPS); thus, SDF-Se had higher immune activity than unmodified SDF, which can be attributed to the synergistic effect of selenium ions and soluble dietary fiber. Consequently, chelating dietary fiber with metallic selenium ions can improve immune function by stimulating peritoneal macrophages to secrete NO.

According to related research, when macrophages are activated, they secrete cytokines, which are crucial biomolecules involved in cell differentiation, maturation, apoptosis, and other vital activities. Cytokines can be widely used in vivo and in vitro to investigate immune activation and immunotoxicity [24, 25]. To confirm the effects of SDF and SDF-Zn on macrophage immune activation, the mRNA expression of cytokines, such as TNF- $\alpha$ , iNOS, IL-1 $\beta$ , IL-10,

and IL-6, was measured using real-time PCR, and the results are shown in Figure 2. TNF- $\alpha$ , as a crucial pleiotropic molecule in macrophages, can not only stimulate macrophages or induce other immune cells to secrete cytokines but also participate in the immune response to kill cancer cells [26]. SDF-Se enhanced the mRNA expression of TNF- $\alpha$  (4.21-fold) in RAW 264.7 cells compared with the control group ( $p < 0.01$ ), thus improving their immune activity. As an essential indicator of cellular immune function, the interleukin (IL) family can directly reflect the strength of cellular immunity, with IL-6, IL-10, and IL-1 $\beta$  being crucial cytokines to improve cellular immunity, and the magnitude of their secretion positively correlates with the strength of immune activity, among which IL-10, as an anti-inflammatory cytokine, plays a role in the negative feedback mechanism, which prevents cell death caused by a severe inflammatory response by inhibiting the overexpression of inflammatory factors, such as TNF- $\alpha$  and IL-6 [27]. The results showed that IL-6, IL-1 $\beta$ , and IL-10 mRNA levels in SDF were similar to those in the control group, indicating that SDFs had less activity in stimulating an immune response. After selenization, the SDF-Se group showed higher cytokine expression, indicating that SDF-Se can enhance Th1- and Th2-type immune responses in macrophages [28]. NO synthase (NOS) comprises neuronal NOS (nNOS), endothelial NOS (eNOS), and induced NOS (iNOS), where iNOS is responsible for most of the NO synthesis [29]. Real-time PCR results show that the production of iNOS mRNA was significantly upregulated upon treatment with 50–200  $\mu\text{g}/\text{mL}$  of SDF-Se, consistent with the NO production results. Subsequently, the results of this experiment demonstrated that selenized SDF could effectively activate macrophages, increasing the secretion of cytokines such as TNF- $\alpha$ , promoting the mRNA expression

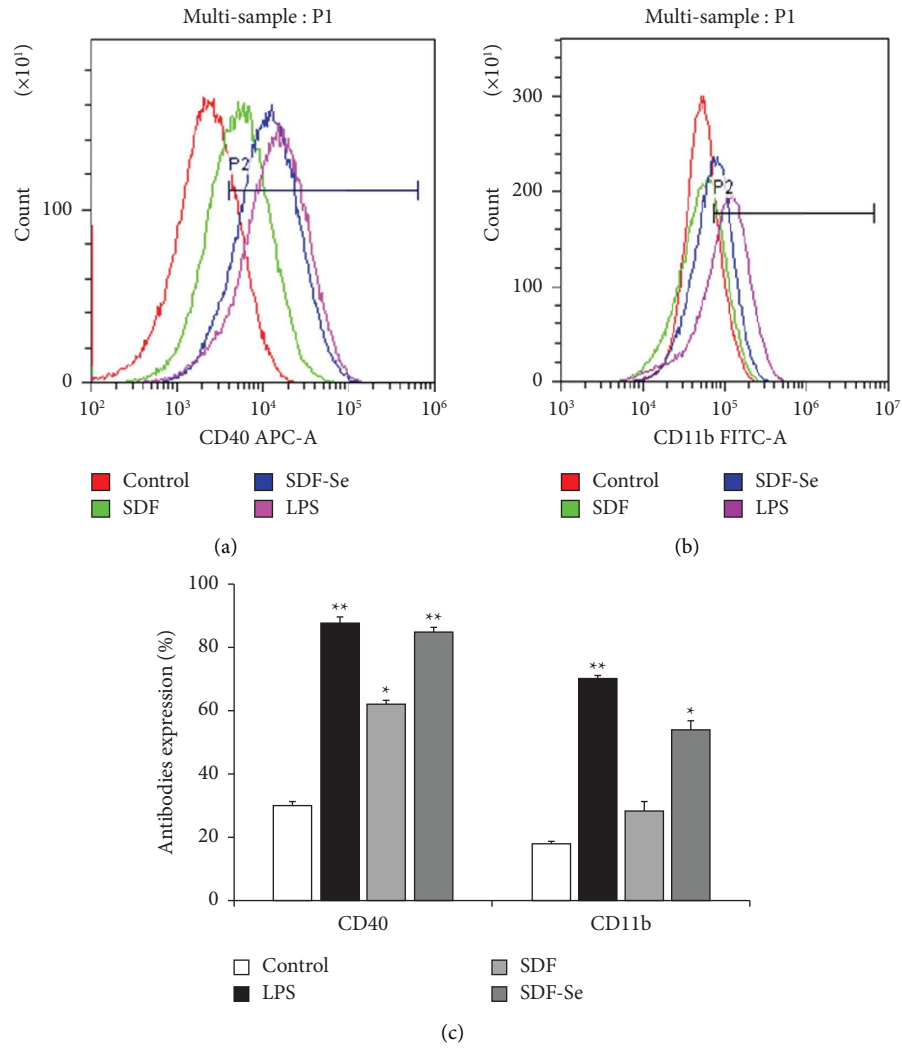


FIGURE 4: The effect of SDF or SDF-Se on the expression of surface molecules in RAW 264.7 cells of (a) CD40, (b) CD11b, and (c) CD40 and CD11b (\*  $p < 0.05$ , \*\*  $p < 0.01$ , and \*\*\*  $p < 0.001$  versus control group).

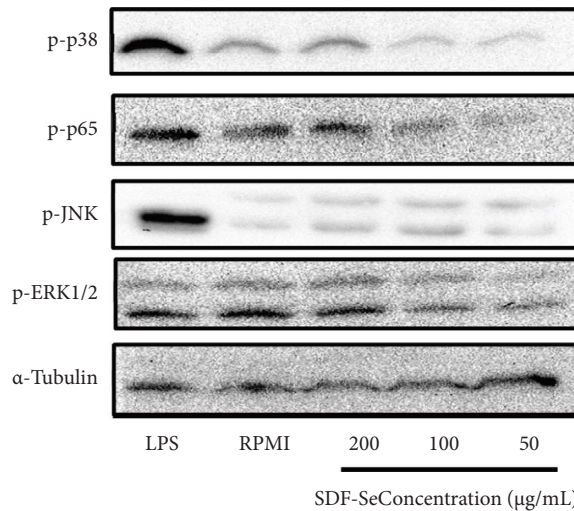


FIGURE 5: The effect of SDF or SDF-Se on the MAPK and NF- $\kappa$ B signaling pathways.



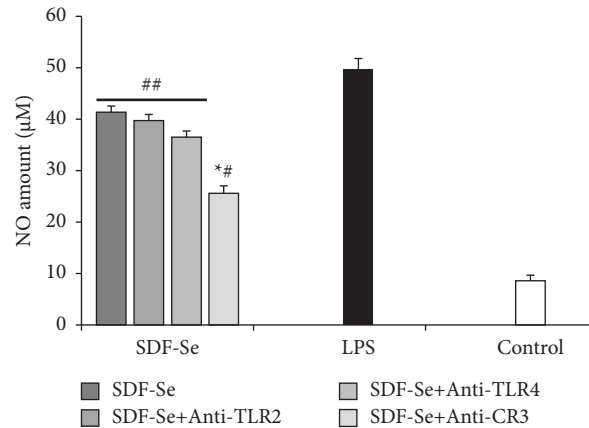


FIGURE 6: The effect of SDF or SDF-Se on specific antibodies against PRR. The RAW 264.7 cell NO production was detected after exposure to the SDF-Se (200 µg/mL). Data are expressed as the mean ± SD. The asterisks indicate statistical changes (ns: not significant; \* $p < 0.05$ , \*\* $p < 0.01$ , and \*\*\* $p < 0.001$  versus SDF-Se group; # $p < 0.05$ , ## $p < 0.01$ , and ### $p < 0.001$  versus control group).

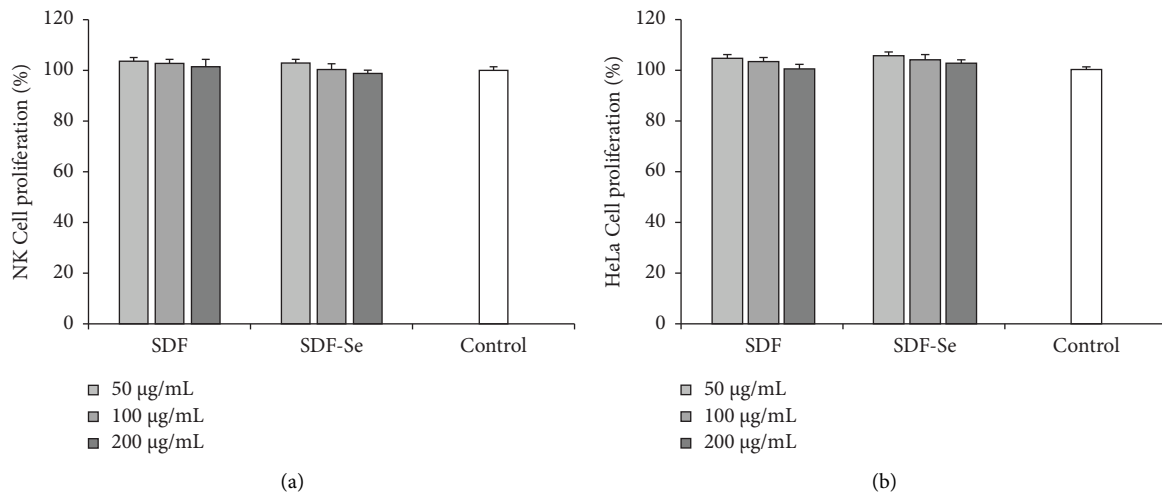


FIGURE 7: The effects of SDF or SDF-Se on NK cell and HeLa cell proliferation: (a) the NK cell proliferation was detected after exposure to the SDF or SDF-Se (50, 100, and 200 µg/mL). (b) The HeLa cell proliferation was detected after exposure to the SDF or SDF-Se (50, 100, and 200 µg/mL). Data are expressed as the mean ± SD. The asterisks indicate statistical changes (ns: not significant; \* $p < 0.05$ , \*\* $p < 0.01$ , and \*\*\* $p < 0.001$  versus control group).

of inducible carbon monoxide synthase (iNOS) in macrophages, and releasing amounts of NO, thereby improving the immunomodulatory function.

ROS, primarily byproducts of the cell, exogenous environment, and other biological reactions, can increase cytokine mRNA expression by modulating molecular signaling pathways, such as the MAPK and NF- $\kappa$ B pathways [30], implying that ROS plays a crucial role in macrophage differentiation and activation. Intracellular ROS accumulation was examined by fluorescence microscopy using the DCFH-DA method after 24 h of SDF and SDF-Se treatment to confirm that SDF-Se regulates immune cell activity by promoting cytokine secretion. There were fewer fluorescently stained cells and weak fluorescence intensity following SDF intervention, indicating that the effect of SDF on immune cell activation was unsatisfactory, which is consistent with previous results (Figure 3). In contrast, the cell

staining effect as ROS accumulation was stronger in the LPS and SDF-Se groups as compared to the control group, indicating that SDF-Se could increase TNF- $\alpha$ , IL-6, and IL-1 $\beta$  gene expression and NO production by increasing ROS accumulation, improving the immunomodulatory function [31].

CD11b and CD40 are crucial inflammatory regulators that not only increase immune cell activities but also induce cytokine expression [32, 33]. Because the CD11b and CD40 surface molecules are widely expressed on the surface of monocytes, granulocytes, macrophages, and NK cells, they were positively correlated with the degree of macrophage activation. The expression of cell surface molecules was measured using cell flowmetry to investigate the immunostimulatory effect of dietary fiber on RAW 264.7 cells before and after modification. As presented in Figure 4, CD11b and CD40 expressions were

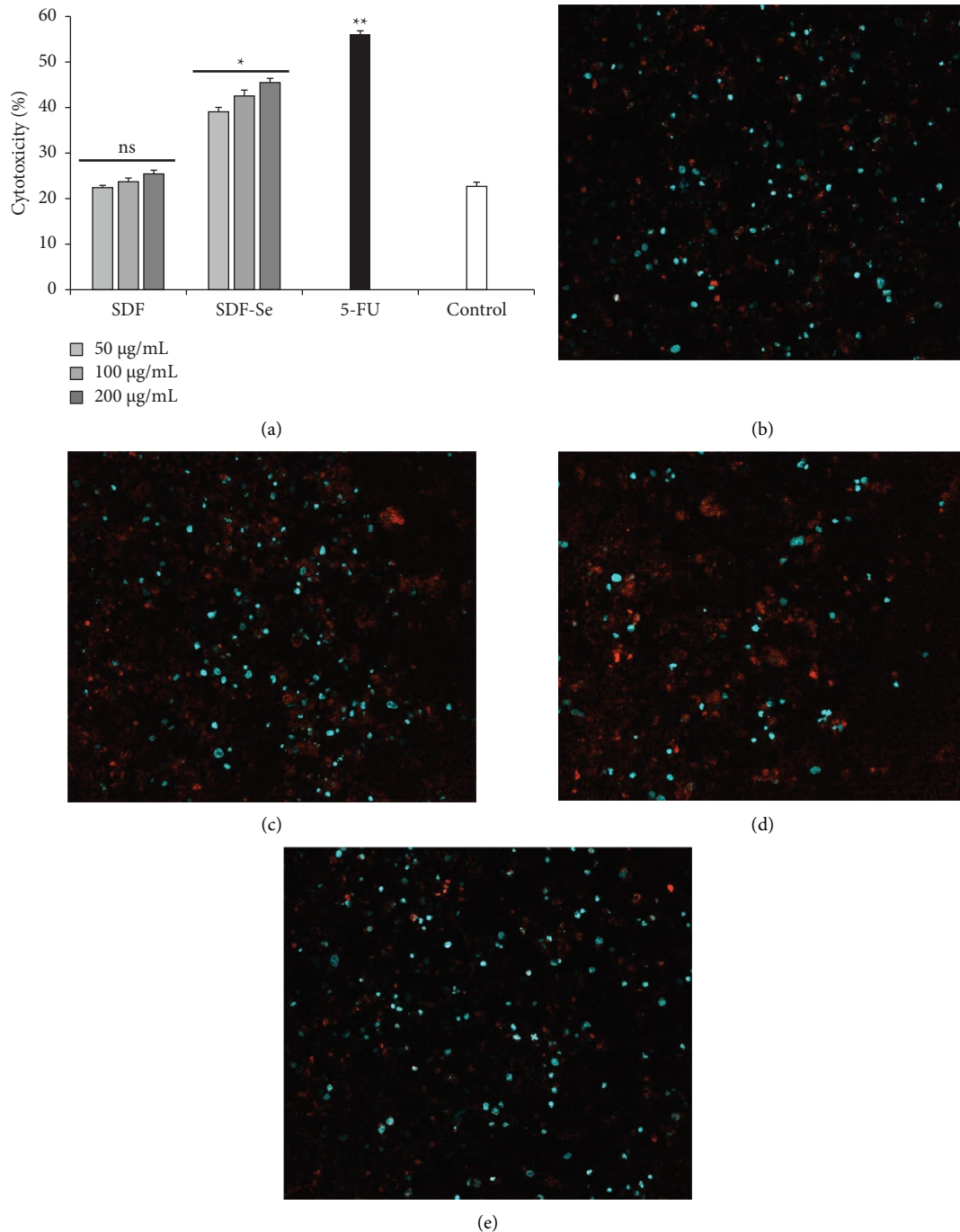


FIGURE 8: The effects of SDF or SDF-Se on NK cell cytotoxicity: (a) the cell cytotoxicity was detected after exposure to the SDF or SDF-Se (50, 100, and 200  $\mu\text{g}/\text{mL}$ ). Quantitative analysis of SDF and SDF-Se (200  $\mu\text{g}/\text{mL}$ ) treated NK cells against HeLa cells: (b) SDF, (c) SDF-Se, (d) 5-FU, and (e) NK cells as control. Data are expressed as the mean  $\pm$  SD. The asterisks indicate statistical changes (ns: not significant; \*  $p < 0.05$ , \*\*  $p < 0.01$ , and \*\*\*  $p < 0.001$  versus control group).

lower in the control group; after incubation with SDF-Se or LPS, approximately 80% of the cells were positive for CD40 markers ( $p < 0.01$ ) and 50% of the cells were positive for CD11b markers, whereas CD40 surface molecule expression was 62.15% in cells treated with SDF ( $p < 0.05$ ); the difference in CD11b markers between the SDF and control groups was not statistically significant, indicating that millet SDF stimulates macrophage

activation by increasing the expression of CD40 surface molecules. SDF-Se, a complex formed by the chelation of SDF with zinc metal ions, regulates the immune response by increasing the expressions of CD11b and CD40 on the surface of immune cells, thereby promoting the accumulation of intracellular ROS and cytokine production and fundamentally enhancing the body's ability to resist external environmental damage.

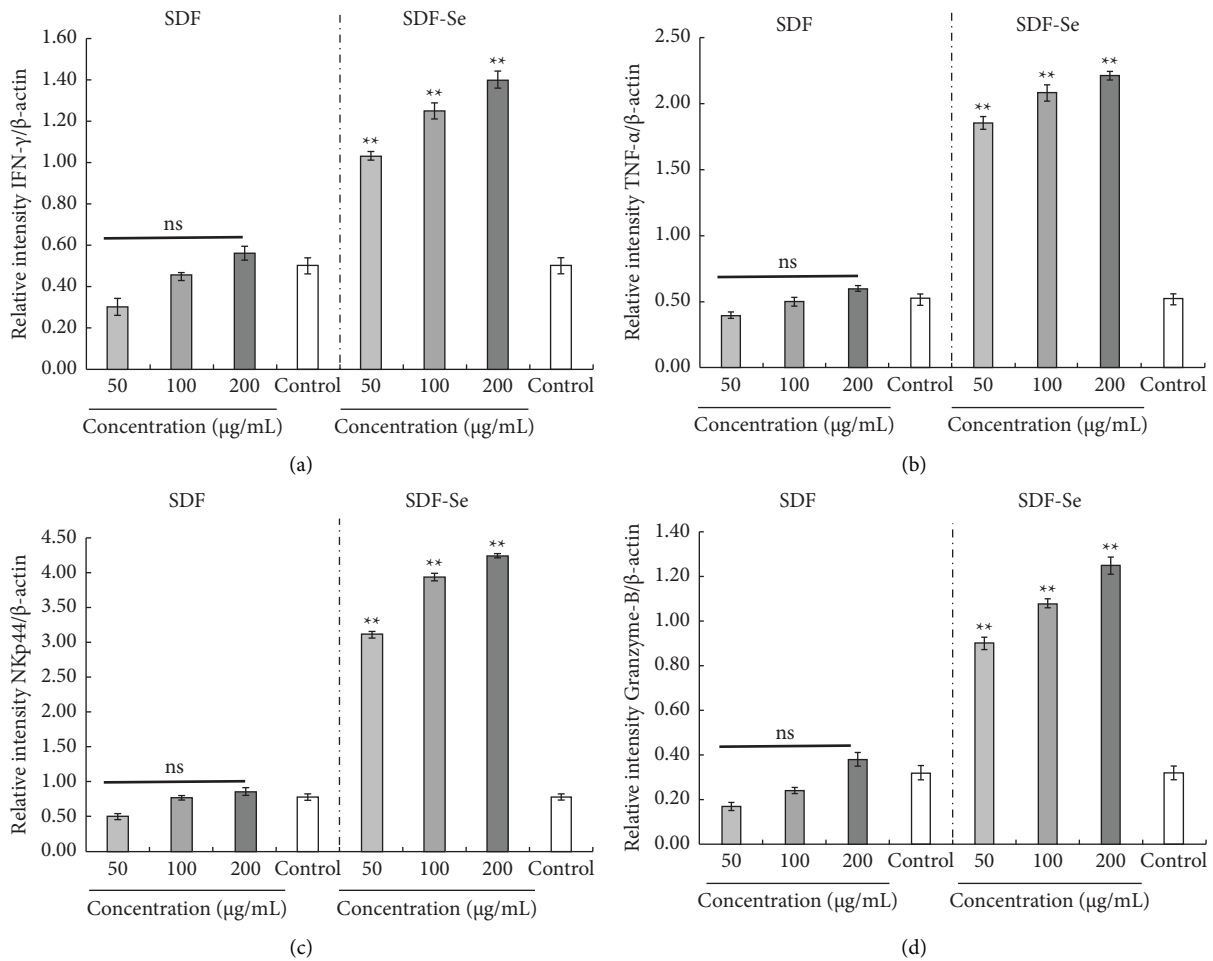


FIGURE 9: The effects of SDF or SDF-Se on mRNA expression. The NK cell mRNA levels were detected after exposure to different concentrations of SDF or SDF-Se (50, 100, and 200  $\mu\text{g}/\text{mL}$ ). Real-time PCR was used to detect the mRNA levels of (a) IFN- $\gamma$ , (b) TNF- $\alpha$ , (c) NKp44, and (d) granzyme-B.  $\beta$ -Actin was used as normalization. Data are expressed as the mean  $\pm$  SD. The asterisks indicate statistical changes (ns: not significant; \* $p < 0.05$ , \*\* $p < 0.01$ , and \*\*\* $p < 0.001$  versus control group).

Related research has demonstrated that mediators such as polysaccharides have immune effects. For example, when macrophages are activated through stimulation, the signals will subsequently activate the key transcription nuclear factor- $\kappa\text{B}$  (NF- $\kappa\text{B}$ ) or MAPK signaling pathways, which induce the expression of inflammatory factors, such as TNF- $\alpha$ , IL-6, IL-1 $\beta$ , and gene transcription in immune cells [34, 35]. The results of cell viability, NO production, and cytokine production confirmed that SDF-Se promoted the immunomodulatory effects of RAW 264.7 cells. To determine whether MAPK and NF- $\kappa\text{B}$  signaling pathways are involved in RAW 264.7 cell activation by SDF-Se, the phosphorylation levels of MAPK and NF- $\kappa\text{B}$  signaling pathway-related proteins were examined using a western blot assay (Figure 5). SDF-Se significantly increased the phosphorylation levels of JNK, ERK, and p38, implying that SDF-Se could promote cytokine and NO production by activating downstream MAPK signaling pathways. We also investigated whether SDF-Se could activate the NF- $\kappa\text{B}$  signaling pathway. When the cells were stimulated with 50,

100, and 200  $\mu\text{g}/\text{mL}$  SDF-Se or 2  $\mu\text{g}/\text{mL}$  LPS, the p65 phosphorylation levels increased, demonstrating that NF- $\kappa\text{B}$  (p65) is a crucial signaling pathway in SDF-Se-induced RAW 264.7 activation.

Macrophages recognize pathogens via pattern recognition receptors (PRRs), including TLRs, CR3, and dectin-1. PRRs bind to pathogen-associated molecular patterns and preserve the motifs expressed on pathogens [36]. This review investigated the roles of TLR2, TLR4, and CR3 receptors in the immune response of SDF-Se-regulating RAW 264.7 cells. Figure 6 shows that treatment with anti-CR3 significantly suppressed NO production ( $p < 0.05$ ) when compared to the SDF-Se group only, but no significant differences were observed when treated with anti-TLR2 or anti-TLR4 ( $p > 0.05$ ). Therefore, SDF-Se binds to CR3 receptors to activate macrophages, triggering a cascade of intracellular signaling response that promotes the phosphorylation of MAPK and NF- $\kappa\text{B}$  signaling pathway-related proteins, arising in transcriptional activation of inflammatory cytokines, and activation of the transcriptional pathways could

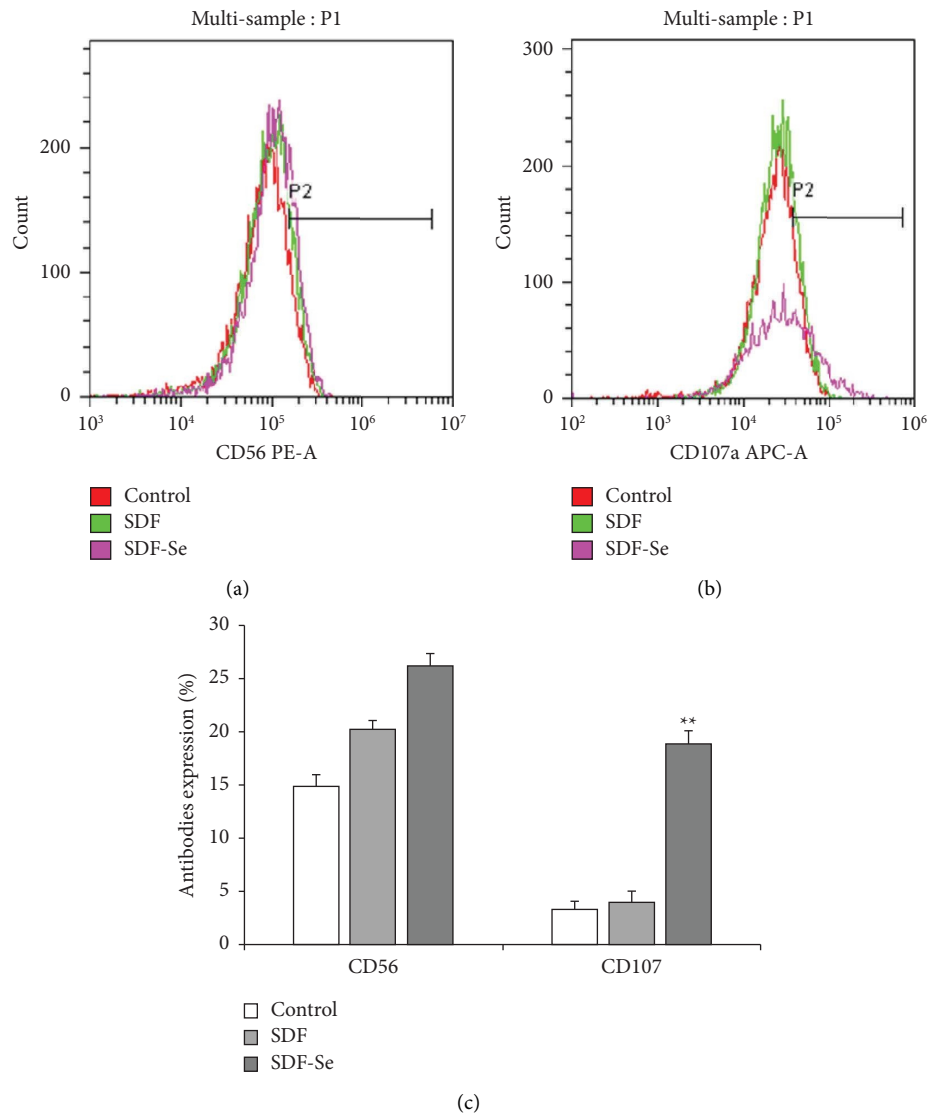


FIGURE 10: The effect of SDF or SDF-Se on the expression of surface molecules in NK cells of (a) CD56, (b) CD107a, and (c) CD56 and CD107a (\* $p < 0.05$ , \*\* $p < 0.01$ , and \*\*\* $p < 0.001$  versus control group).

result in the expression of proinflammatory cytokines (TNF- $\alpha$  and IL-6) as well as inducible nitric oxide synthase (iNOS) [37].

NK cells play a critical role in innate immunity as lymphocytes that recognize and eliminate viral infections and tumor cells, and their cytotoxicity to cancer cells is a marker of NK cell activation [38, 39]. The cytotoxicity of SDF- and SDF-Se-stimulated NK cells inducing apoptosis in target cells HeLa was assessed using the EZ-Cytox new cell viability assay (Figure 8(a)). The SDF-treated NK cell exhibited 22.15–25.34% of cytotoxicity against HeLa cells, which was a similar level to the NK cells alone (22.58%), while NK cells activated by SDF-Se stimulation had a substantial inhibitory impact on HeLa cell viability and exhibited agent dependence (cytotoxicity increased from 38.94% to 45.36% as SDF-Se concentration increased) lower than 5-Fu (a positive control). The NK cell cytotoxicity level was confirmed by the CQ1 analysis (cell nuclei were

visualized by DAPI in blue, whereas cells undergoing necrosis were stained by PI in red). HeLa cells without any addition of NK cells served as a control, which showed a large number of live cancer cells (Figure 8(e)); when SDF-Se and 5-FU were coincubated with NK cells for 4 h, the number of live cells significantly decreased (Figures 8(c) and 8(d)), and a significant number of live cancer cells was observed in the cells treated with SDF (Figure 8(b)), showing good agreement with the abovementioned NK cell cytotoxicity results. This suggests that after modification with Se ions, dietary fiber can significantly stimulate NK cell activation and increase cytotoxicity in target cancer cells.

Related research has found that when NK cells are activated and express cytotoxicity against cancer cells, they secrete various chemokines and cytokines, such as IFN- $\gamma$  and TNF- $\alpha$ , cytoplasmic granules, such as granzyme-B, and various surface activating receptors, such as NKp44. It has been reported that NK cells clear virus-infected cells and

tumor cells by releasing perforins and granzymes, while interferon  $\gamma$  (IFN- $\gamma$ ) and tumor necrosis factor  $\alpha$  (TNF- $\alpha$ ) are produced to induce apoptosis in target cells, so the symbol of NK is activated and becomes more cytotoxic to tumor cells in the secretion of IFN- $\gamma$ , perforin, granzyme-B, and expressions of NKp30 and TLR4 [40, 41]. A similar trend was observed in this study (Figure 9). The mRNA expression levels of IFN- $\gamma$  and TNF- $\alpha$  were increased (upregulated 2.8- and 4.25-fold compared to the control) with a high concentration of SDF-Se treatment, and a similar trend was observed for the mRNA expression levels of granzyme-B and NKp44, which were increased (upregulated 3.9- and 3.1-fold compared with the control) ( $p < 0.01$ ). However, SDF treatment resulted in similar levels of gene expression as the control group, revealing that SDF-Se could possibly activate NK cells compared to SDF.

According to previous research, activated NK cells are crucial for tumor clearance and innate immunity; therefore, investigating the influence of external factors on NK cell activation is essential. CD56, a neural cell-associated adhesion molecule, is a functional indicator of NK cells [42]. CD56 expression on the surface of NK cells increased slightly after SDF pretreatment compared to the control group; however, the difference was not statistically significant, whereas CD56 expression increased dramatically after SDF-Se intervention (Figure 10(a)). As a marker of NK cell functional activity, CD107a can be used to identify activated NK cells. Furthermore, CD107a expression has been linked to cytokine secretion and NK cell-mediated target cell lysis [43]. Cell flowmetry was used to determine the expression of CD107a on NK cell surfaces following treatment with different samples. SDF-Se considerably improved the CD107a expression, while SDF and the control groups had similar levels (Figure 10(b)), indicating that Se-ion-chelating SDF could activate transcription factors and alter the gene expression involved in promoting IFN- $\gamma$  and TNF- $\alpha$  secretion and CD56 and CD107a expressions.

## 5. Conclusion

Soluble dietary fiber was extracted from millet and modified with selenium ions to create SDF-Se. RAW 264.7 cells were cocultured to determine the immune activity effect of SDF-Se on macrophages. The results demonstrated that SDF-Se significantly increased NO production, ROS and cytokines secretion, and the expression of the cell surface molecules CD11b and CD40 when compared to SDF. The secretion of IFN- $\gamma$ , TNF- $\alpha$ , and granzyme-B and the expression of NK cell surface molecules CD56 and CD107a were all significantly increased when SDF-Se was used to activate NK cells against HeLa cells. These results suggest that SDF-Se can increase the immune function by inducing the activation of NK cells and macrophages. Nevertheless, further research is required to explore the molecular mechanism between immune cells and the structural properties of SDF-Se.

## Data Availability

The data used to support the findings of this study are included within the paper.

## Conflicts of Interest

The authors declare that there are no conflicts of interest.

## Authors' Contributions

Y F G was involved in methodology, data analysis, drawing charts, and writing the original draft and editing the manuscript; C H W visualized the study investigated and validated the data; D Z L validated the data and performed formal analysis; L K C reviewed and edited the manuscript and was responsible for funding acquisition. All authors have read and agreed to publish the current version of the manuscript. Yunfei Ge and Chunhong Wei contributed equally to this work.

## Acknowledgments

This study was funded by the National Key Research and Development Plan (grant no. 2017YFD0401203) and the Heilongjiang Bayi Agricultural University graduate innovation research project (grant no. YJSCX2018-Y53).

## References

- [1] K. M. Brown and J. R. Arthur, "Selenium, selenoproteins and human health: a review," *Public Health Nutrition*, vol. 4, no. 2b, pp. 593–599, 2001.
- [2] U. Tinggi, "Selenium: its role as antioxidant in human health," *Environmental Health and Preventive Medicine*, vol. 13, no. 2, pp. 102–108, 2008.
- [3] F. Chen and G. L. Huang, "Preparation and immunological activity of polysaccharides and their derivatives," *International Journal of Biological Macromolecules*, vol. 112, pp. 211–216, 2018.
- [4] N. Chen, C. Zhao, and T. Zhang, "Selenium transformation and selenium-rich foods," *Food Bioscience*, vol. 40, Article ID 100875, 2021.
- [5] M. Roman, P. Jitaru, and C. Barbante, "Selenium biochemistry and its role for human health," *Metallomics*, vol. 6, no. 1, pp. 25–54, 2014.
- [6] B. Kaleta, A. Roszczyk, M. Zych et al., "Selective biological effects of selenium-enriched polysaccharide (Se-Le-30) isolated from *lentinula edodes* mycelium on human immune cells," *Biomolecules*, vol. 11, no. 12, p. 1777, 2021.
- [7] S. Qiu, J. Chen, T. Qin et al., "Effects of selenylation modification on immune-enhancing activity of garlic polysaccharide," *PLoS One*, vol. 9, no. 1, 2014.
- [8] H. Xu, *Selenium: Its Chemistry, Biochemistry and Application in Life Science*, Huzhong University of Science & Technology Press, Wuhan, China, 1994.
- [9] Q. Hu and B. Guo, "The influence of spirulina selenium polysaccharide on immune function," *Journal of Chinese Marine Drugs*, vol. 5, pp. 20–29, 2001.
- [10] C. Wang, R. Song, S. Wei et al., "Modification of insoluble dietary fiber from ginger residue through enzymatic treatments to improve its bioactive properties," *LWT-Food Science and Technology*, vol. 125, Article ID 109220, 2020.
- [11] Z. Xu, X. Xiong, Q. Zeng et al., "Alterations in structural and functional properties of insoluble dietary fibers-bound phenolic complexes derived from lychee pulp by alkaline hydrolysis treatment," *LWT-Food Science and Technology*, vol. 127, Article ID 109335, 2020.

- [12] N. Zhang, C. H. Huang, and S. Y. Ou, "In vitro binding capacities of three dietary fibers and their mixture for four toxic elements, cholesterol, and bile acid," *Journal of Hazardous Materials*, vol. 186, no. 1, pp. 236–239, 2011.
- [13] M. Moczowska, S. Karp, Y. Niu, and M. A. Kurek, "Enzymatic, enzymatic-ultrasonic and alkaline extraction of soluble dietary fibre from flaxseed—a physicochemical approach," *Food Hydrocolloids*, vol. 90, pp. 105–112, 2019.
- [14] H. Bader Ul Ain, F. Saeed, M. U. Arshad, N. Ahmad, M. A. Nasir, and R. M. Amir, "Modification of barley dietary fiber through chemical treatments in combination with thermal treatment to improve its bioactive properties," *International Journal of Food Properties*, vol. 21, no. 1, pp. 2491–2499, 2018.
- [15] M. Staaf, Z. N. Yang, E. Huttunen, and G. Widmalm, "Structural elucidation of the viscous exopolysaccharide produced by *Lactobacillus helveticus* Lb161," *Carbohydrate Research*, vol. 326, no. 2, pp. 113–119, 2000.
- [16] W. H. Wang, F. Kou, J. Wang, Z. G. Quan, S. T. Zhao, and Y. F. Wang, "Pretreatment with millet-derived selenylated soluble dietary fiber ameliorates dextran sulfate sodium-induced colitis in mice by regulating inflammation and maintaining gut microbiota balance," *Frontiers in Nutrition*, vol. 9, Article ID 928601, 2022.
- [17] W. Z. Liao, Y. J. Lu, J. N. Fu, Z. X. Ning, J. G. Yang, and J. Y. Ren, "Preparation and characterization of *Dictyophora indusiata* polysaccharide-Zinc complex and its augmented antiproliferative activity on human cancer cells," *Journal of Agricultural and Food Chemistry*, vol. 63, no. 29, pp. 6525–6534, 2015.
- [18] P. Y. Gao, J. Bian, S. H. Xu, C. F. Liu, Y. Q. Sun, and G. L. Zhang, "Structural features, selenization modification, antioxidant and anti-tumor effects of polysaccharides from alfalfa roots," *International Journal of Biological Macromolecules*, vol. 149, pp. 207–214, 2020.
- [19] K. Yelithao, U. Surayot, C. Lee et al., "Studies on structural properties and immune-enhancing activities of glycomannans from *Schizophyllum commune*," *Carbohydrate Polymers*, vol. 218, pp. 37–45, 2019.
- [20] M. X. Wang, C. Y. Fu, M. C. Zhang, Y. X. Zhang, and L. Cao, "Immunostimulatory activity of soybean hull polysaccharide on macrophages," *Experimental and Therapeutic Medicine*, vol. 23, no. 6, 2022.
- [21] Y. X. Yang, J. L. Chen, L. Lei, F. Li, Y. Y. Tang, and Y. Q. Yuan, "Acetylation of polysaccharide from *Morchella angusticeps* peck enhances its immune activation and anti-inflammatory activities in macrophage RAW264.7 cells," *Food and Chemical Toxicology*, vol. 125, pp. 38–45, 2019.
- [22] Q. Y. Liu, Y. M. Yao, S. W. Zhang, and Z. Y. Sheng, "Astragalus polysaccharides regulate T cell-mediated immunity via CD11c high CD45RB low DCs in vitro," *Journal of Ethnopharmacology*, vol. 136, no. 3, pp. 457–464, 2011.
- [23] A. Pautz, J. Art, S. Hahn, S. Nowag, C. Voss, and H. Kleinert, "Regulation of the expression of inducible nitric oxide synthase," *Nitric Oxide*, vol. 23, no. 2, pp. 75–93, 2010.
- [24] S. Bahramzadeh, M. Tabarsa, S. G. You, K. Yelithao, V. Klochkov, and R. Ilfat, "An arabinogalactan isolated from *Boswellia carterii*: Purification, structural elucidation and macrophage stimulation via NF- $\kappa$ B and MAPK pathways," *Journal of Functional Foods*, vol. 52, pp. 450–458, 2019.
- [25] R. D. Divate and Y. C. Chung, "In vitro and in vivo assessment of anti-inflammatory and immunomodulatory activities of *Xylaria nigripes* mycelium," *Journal of Functional Foods*, vol. 35, pp. 81–89, 2017.
- [26] K. S. Siveen and G. Kuttan, "Role of macrophages in tumour progression," *Immunology Letters*, vol. 123, no. 2, pp. 97–102, 2009.
- [27] D. S. Chi, M. Qui, G. Krishnaswamy, C. Li, and W. Stone, "Regulation of nitric oxide production from macrophages by lipopolysaccharide and catecholamines," *Nitric Oxide*, vol. 8, no. 2, pp. 127–132, 2003.
- [28] Y. Luo, Z. Ren, R. N. Bo, X. P. Liu, J. W. Zhang, and R. H. Yu, "Designing selenium polysaccharides-based nanoparticles to improve immune activity of *Hericium erinaceus*," *International Journal of Biological Macromolecules*, vol. 143, pp. 393–400, 2020.
- [29] X. Xu, M. Yasuda, M. Mizuno, and H. Ashida, " $\beta$ -Glucan from *Saccharomyces cerevisiae* reduces lipopolysaccharide-induced inflammatory responses in RAW264.7 macrophages," *Biochimica et Biophysica Acta (BBA)-General Subjects*, vol. 1820, no. 10, pp. 1656–1663, 2012.
- [30] Q. Yu, S. P. Nie, J. Q. Wang et al., "Toll-like receptor 4-mediated ROS signaling pathway involved in *Ganoderma atrum* polysaccharide-induced tumor necrosis factor- $\alpha$  secretion during macrophage activation," *Food and Chemical Toxicology*, vol. 66, pp. 14–22, 2014.
- [31] G. Mao, Y. Ren, Q. Li, H. Wu, D. Jin, and T. Zhao, "Anti-tumor and immunomodulatory activity of selenium (Se)-polysaccharide from Se-enriched *Grifola frondosa*," *International Journal of Biological Macromolecules*, vol. 82, pp. 607–613, 2016.
- [32] D. F. Huang, S. P. Nie, L. M. Jiang, and M. Y. Xie, "A novel polysaccharide from the seeds of *Plantago asiatica* L. induces dendritic cells maturation through toll-like receptor 4," *International Immunopharmacology*, vol. 18, no. 2, pp. 236–243, 2014.
- [33] R. M. Andrade, M. Wessendarp, M. J. Gubbels, B. Striepen, and C. S. Subauste, "CD40 induces macrophage anti-*Toxoplasma gondii* activity by triggering autophagy-dependent fusion of pathogen-containing vacuoles and lysosomes," *Journal of Clinical Investigation*, vol. 116, no. 9, pp. 2366–2377, 2006.
- [34] M. Muzio, G. Natoli, S. Sacconi, M. Levrero, and A. Mantovani, "The human toll signaling pathway: divergence of nuclear factor  $\kappa$ B and JNK/SAPK activation upstream of tumor necrosis factor receptor-associated factor 6 (TRAF6)," *Journal of Experimental Medicine*, vol. 187, no. 12, pp. 2097–2101, 1998.
- [35] Y. H. Xie, L. X. Wang, H. Sun, Y. X. Wang, Z. B. Yang, and G. G. Zhang, "Polysaccharide from alfalfa activates RAW 264.7 macrophages through MAPK and NF- $\kappa$ B signaling pathways," *International Journal of Biological Macromolecules*, vol. 126, pp. 960–968, 2019.
- [36] X. Q. Li and W. Xu, "TLR4-mediated activation of macrophages by the polysaccharide fraction from *Polyporus umbellatus* (pers.) Fries," *Journal of Ethnopharmacology*, vol. 135, pp. 1–6, 2011.
- [37] M. Yin, Y. Zhang, and H. Li, "Advances in research on immunoregulation of macrophages by plant polysaccharides," *Frontiers in Immunology*, vol. 10, p. 145, 2019.
- [38] D. S. Chen and I. Mellman, "Elements of cancer immunity and the cancer-immune set point," *Nature*, vol. 541, no. 7637, pp. 321–330, 2017.
- [39] Q. Huang, M. Huang, F. Meng, and R. Sun, "Activated pancreatic stellate cells inhibit NK cell function in the human pancreatic cancer microenvironment," *Cellular and Molecular Immunology*, vol. 16, no. 1, pp. 87–89, 2019.

- [40] G. L. Paulina, B. C. Alejandro, H. F. Georgina et al., "Increase of IFN- $\gamma$  and TNF- $\alpha$  production in CD107a + NK-92 cells co-cultured with cervical cancer cell lines pre-treated with the HO-1 inhibitor," *Cancer Cell International*, vol. 100, 2014.
- [41] H. Lu, Y. Yang, E. Gad et al., "TLR2 agonist PSK activates human NK cells and enhances the antitumor effect of HER2-targeted monoclonal antibody therapy," *Clinical Cancer Research*, vol. 17, no. 21, pp. 6742–6753, 2011.
- [42] A. Poli, T. Michel, M. Thérésine, E. Andrès, F. Hentges, and J. Zimmer, "CD56<sup>bright</sup> natural killer (NK) cells: an important NK cell subset," *Immunology*, vol. 126, no. 4, pp. 458–465, 2009.
- [43] G. Alter, J. M. Malenfant, and M. Altfeld, "CD107a as a functional marker for the identification of natural killer cell activity," *Journal of Immunological Methods*, vol. 294, no. 1-2, pp. 15–22, 2004.